

## **Biomimetic Self-Healing Metals**

Michele V. Manuel\* and Gregory B. Olson†

*Department of Materials Science and Engineering, Northwestern University, 2220  
Campus Drive, Evanston, IL 60208*

\*Tel: 1-847-491-3689 †Tel: 1-847-491-2847

Fax: 1-847-491-7820

\*Email: m-manuel@northwestern.edu †Email: g-olson@northwestern.edu

### **ABSTRACT**

Novel self-healing alloy composites have been designed to address the need for self-repairable high-strength structural materials. A systems-based materials design approach using computational design tools was used to design a multifunctional biomimetic composite that can repair structural damage. The self-healing composite consists of a controlled-melting alloy matrix reinforced by thermodynamically compatible shape memory alloy (SMA) wires. When heat is applied to the composite after damage, the embedded SMA wires apply a compressive force which produces crack closure and clamping. The matrix alloy is designed to become partially molten at the healing temperature to reverse damage induced plasticity and provide crack welding. Feasibility tests on prototype composites show greater than 95% recovery of ultimate tensile strength after crack healing.

### **INTRODUCTION**

There is an increasing demand for greater reliability in load-bearing engineering structures. Often failure of these structures could endanger lives and are increasingly too costly to replace. There has always been a need and a vision of the future which includes structures with the ability to self-heal. Research efforts in self-healing materials have been largely based on polymeric and cementitious based composites [1-3] with very little discussion of metallic-based self-healing materials [4].

This paper focuses on the design, fabrication, and testing of proof-of-concept self-healing Sn-based metal-matrix composites (MMCs) reinforced with shape memory alloy (SMA) wires. The mechanical properties of the composite are investigated to demonstrate increased toughness and self-healing through

strength recovery. A simple analytical model is also described which provides a theoretical framework for composite design.

The concept of self-healing materials has largely been inspired by the success of biological systems to adapt to their environment. Researchers have used the term biomimetics to describe engineering design that imitates nature. The unique behavior in these systems has been found by previous investigators to arise from the innate structure-property relationships in these materials [5, 6]. The relationships that are mimicked in the self-healing composite can be found in complex biological systems such as the nacre of mollusks, which demonstrate composite toughening [7, 8], and primitive systems like bacteria, which demonstrate the shape memory effect [9].

## **CONCEPTUAL DESIGN**

A proof-of-concept composite which demonstrates crack closure and self-healing to maximize strength recovery has been designed. The composite consists of an alloy matrix and SMA wires as the reinforcements. The healing temperature was defined by a composition which minimizes the thermal budget, allows for robust melting behavior and provides structural stability of the composite during healing. When the alloy reaches the healing temperature, a clamping force is applied by the SMA wire reinforcements and a fraction of the matrix liquefies to weld the crack surfaces of bridged cracks together (see Figure 1). This design will utilize a thermodynamics-based systems approach that will ensure that the SMA reinforcement and the matrix are thermodynamically compatible at processing and operating temperatures.

The optimization of the complex, multilevel structures in this composite would be difficult to obtain from a trial-and-error approach, therefore, materials design framed by a systems engineering approach [10] was used in designing the self-healing alloy composite. The flow-block diagram in Figure 2 illustrates the hierarchical nature of the system, interactions between subsystems and an overall objective. Specific property objectives such as memory healing, strength recovery and toughness can be optimized by analyzing subsystems and their interactions. The interactions outline the pathway for composite design.

## **DESIGN MODELING AND SUBSYSTEM CHARACTERIZATION**

The principal computational design tool used in this research is the Thermo-Calc software system developed by the Royal Institute of Technology. The thermochemical database used for the design of the alloy matrix was developed by the National Institute of Standards and Technology (NIST). The database contains a thermodynamic assessment of solder systems and the phase equilibria obtained from the software was used as a roadmap for alloy design.

The self-healing composite consists of a Sn-13at%Bi alloy matrix embedded with continuous uniaxially oriented equiatomic TiNi SMA wires. The low melting temperature, castability and low cost of the Sn-Bi alloy system make it ideal for use as the matrix for the proof-of-concept composite. The healing temperature was set by designing for a composition that maximizes  $\Delta T$ , the difference between the liquidus and eutectic temperature, which offers the most gradual melting for robust processing control. The composition of the matrix was designed for a healing temperature of 169°C, with a 20% liquid fraction. The calculated Sn-Bi phase diagram in Figure 3 displays the composition of interest which is followed by the melting characteristics of the matrix alloy. The green box indicates a tolerance level of +/- 5% liquid fraction corresponding to a possible range of healing temperatures from 161 to 177°C.

### **Analytical Thermomechanical Model Development**

The thermomechanical design of the composite to achieve crack closure and crack clamping requires fundamental knowledge of the behavior of the constituent materials. This knowledge leads to predictive capabilities that aid composite design. To efficiently predict composite behavior, a constitutive model of the composite was developed by the Advanced Materials Laboratory at Northwestern University [11]. The matrix behavior was modeled as a simple two-dimensional elastic-plastic material and the wires were modeled using a one-dimensional constitutive model developed by Brinson [12]. Using a user subroutine, the Brinson one-dimensional SMA model was integrated into the commercial ABAQUS finite element analysis code. The model allows users to input material parameters for each constituent composite phase to understand the

evolution of stress in the composite and to ultimately predict the thermomechanical behavior of the composite. Motivated by Brinson's numerical simulation, the authors developed a simple analytical model to predict the thermomechanical behavior of the composite as a function of volume fraction of reinforcement and temperature.

If there is no pre-strain in the SMA wires and no ductility in the matrix, the deformation which occurs during fracture induces a strain in the SMA. During heating, the SMA wires will begin reversion from martensite to austenite under a stress free state at the austenite start temperature ( $A_s$ ) and complete the shape recovery at the austenite finish temperature ( $A_f$ ), and only crack closure would be achieved. However, if the composite is designed to reverse flow the matrix and reverse the plastic deformation caused by specimen fracture, the addition of pre-strained SMA wires or a moderately ductile matrix (which will induce transformation in the SMA wires via plastic flow of the matrix) will be needed to produce a crack clamping force. Upon heating, with the addition of pre-strained SMA wires or a ductile matrix, the SMA wires will begin to revert under a stress free state at the  $A_s$  temperature until the crack surfaces come into contact at a temperature between the  $A_s$  and  $A_f$ . When crack closure is achieved, crack clamping begins as the SMA wires begin to apply a compressive stress to the matrix to reverse the plastic deformation, while promoting diffusional welding. This process causes the SMA wires to become constrained by the matrix and a reversion stress,  $\sigma_R$ , will develop during heating. The stress increases the stability of the martensite phase and the transformation temperatures shift to higher temperatures at a rate of  $d\sigma/dT$ . Perkins [13] has shown that the rate at which  $\sigma_R$  increases can be approximated by  $d\sigma/dT$  and that  $\sigma_R$  will increase until it is relieved by internal plastic deformation (yielding in the SMA wires), external plastic deformation (yielding in the matrix) or removal of the constraint [14]. This has also been verified by the numerical simulation developed by Brinson *et al.*[11]. For design purposes, a design constraint is invoked such that the maximum value of  $\sigma_R$  must always be lower than the flow stress of the austenite phase,  $\sigma_{Flow}$ , i.e.

$$\sigma_R < \sigma_{Flow} \quad (1)$$

In order to meet this design constraint, the composite is designed with a volume fraction of reinforcement that will cause the matrix to yield, such that the

constraint on the wires is released as a function of temperature to prevent plastic flow of the SMA wires.

At equilibrium, a balance condition exists such that the applied forces in the interfacial boundary layer between the SMA wires and the matrix are equal and opposite in direction:

$$\sigma_{SMA}V_f - \sigma_{Matrix}(1 - V_f) = 0. \quad (2)$$

The terms  $\sigma_{SMA}$  and  $\sigma_{Matrix}$  represents the recovery stress of the SMA wires and the stress in the matrix, respectively, and  $V_f$  represents the volume fraction of SMA wires in the matrix. For design purposes, the recovery stress,  $\sigma_{SMA}$ , applied by the SMA wires can be approximated by the flow stress of the parent phase, austenite ( $\sigma_{Flow}$ ) [13, 15]. Given the design constraint that the SMA wires must yield the matrix to prevent the plastic deformation of the SMA, we set  $\sigma_{Matrix}$  equal to the matrix compressive yield strength ( $\sigma_{MCYS}$ ), such that

$$\sigma_{MCYS} \left( \frac{V_f}{1 - V_f} \right) < \sigma_{Flow}. \quad (3)$$

and the design constraints are satisfied when (1) is equal to (3),

$$\sigma_R = \sigma_{MCYS} \left( \frac{V_f}{1 - V_f} \right). \quad (4)$$

### Subsystem Characterization

To fabricate the matrix alloy, elemental tin (purity, 99.8%) and bismuth (purity, 99.99%) obtained from Alfa Aesar were weighed out to achieve a composition of Sn-13at%Bi and melted in a furnace at 300°C. The melt was cast into pre-heated graphite molds to slow solidification and to facilitate casting.

The SMA wires used in this research were obtained from Memry Corporation were 191 microns in diameter and received in the cold-worked state. Prior to casting, the SMA wires were annealed for 3 hours at 500°C in an evacuated Pyrex tube to increase transformation temperatures. The measured transformation temperatures after heat treatment using a DSC were  $A_s = 88^\circ\text{C}$  and  $A_f = 105^\circ\text{C}$ . The slope of the locus of points representing the stress dependent austenite transformation temperatures,  $d\sigma/dT$ , was measured by analyzing the change in electrical resistance as a function of temperature under a constant load.  $d\sigma/dT$  was determined to be 10 MPa/°C.

Compression tests were performed on the matrix alloy to determine the compressive yield strength as a function of temperature. Samples were heat treated at the healing temperature and time to eliminate casting effects and then machined to a length/diameter ratio of 1.5. Tensile tests were performed on the SMA wires to determine the orientation, transformation and parent phase flow stresses as a function of temperature. Tensile and compression tests were carried out on an MTS Sintech 20/G in a range of temperatures from room temperature to 169°C

### **Analytical Thermomechanical Model Results**

The schematic in Figure 4 displays the evolution of  $\sigma_R$  within the SMA wires as a function of temperature. The orange lines represent the path of the reversion stress. The curve,  $\sigma_{MCYS}(T, V_f=1\%)$ , represents the matrix compressive yield stress that is constraining the 1% volume fraction of SMA wires. The arrow on the  $\sigma_{MCYS}(T, V_f=1\%)$  curve shows the shift in the curve with increasing volume fraction of reinforcement. Once the reversion stress reaches  $\sigma_{MCYS}(T, V_f=1\%)$  such that (1) and (3) are satisfied, the stress in the wire will continue to follow  $\sigma_{MCYS}(T, V_f=1\%)$  until the healing temperature,  $T_{Heal}$  at 169°C. According to the schematic, the minimum volume fraction of SMA wires needed to satisfy equations (1) and (3) is 1%

## **DESIGN INTEGRATION AND PROOF-OF-CONCEPT EVALUATION**

Sn-based self-healing proof-of-concept composites were fabricated using a Sn-13at%Bi matrix and equiatomic NiTi SMA wires. The SMA wire reinforcements were continuous and uniaxially oriented with a volume fraction of 1% in the matrix. Prior to casting, the wires were sputter coated with 5nm of gold to increase wettability of the wire surface during casting and then were threaded through customized clamps which held the wires in tension during casting.

All composite tensile specimens were machined to a gauge length of 25mm and a gauge width of 6mm. Tensile tests were performed to assess the mechanical behavior of the composite and matrix alloys. Figure 5a displays the typical stress-strain curves for the Sn-Bi unreinforced matrix alloy and the Sn-Bi reinforced proof-of-concept composite. The composite displays a 500% increase

in uniform ductility in comparison to the unreinforced prototype alloy which is evidence of significant composite toughening.

To demonstrate healing efficiency, tensile tests were performed on the composites at room temperature until complete matrix failure. After failure, the specimens were removed from the tensile testing apparatus and heat treated at 169°C for 24 hours in evacuated Pyrex tubes to heal the crack. Following crack healing, the specimens were again tensile tested to failure to determine the amount of strength recovery.

When the samples were tensile tested after the healing cycle, greater than 95% ultimate tensile strength recovery was achieved (see Figure 5b). The improvement in strength recovery was offset by a reduction in uniform ductility. A possible cause for the reduction in uniform ductility after the healing cycle is oxidation and embrittlement of the crack surfaces during healing. Pictures of the samples prior to the healing cycle and post-healing cycle showing a healed sample are displayed in Figure 6.

## **SUMMARY AND FUTURE DIRECTIONS**

A thermodynamics-based systems design approach has been used to design and demonstrate a proof-of-concept self-healing Sn-based metal-matrix composite reinforced by 1 vol. % of NiTi SMA wires. Mechanical testing of the composite shows a 500% increase in uniform ductility. After a healing treatment of 169°C for 24 hours, the composites display greater than 95% recovery of ultimate tensile strength. From these results, it is concluded that an alloy composite reinforced with SMA wires can be designed for increased toughness and self-healing. Furthermore, an analytical model motivated by numerical simulations was presented to analyze the evolution of internal stress in the SMA wires and determine the optimal volume fraction of reinforcement needed for self-healing. Proof-of-concept composites were designed and fabricated based on results from the model, and the model was validated through demonstrations of successful healing treatments.

Work is currently ongoing to design a high specific strength precipitation strengthened magnesium-based self-healing metal-matrix composite reinforced by precipitation strengthened SMA wires. The high specific strength of magnesium-based alloys makes it an attractive option as a lightweight structural load-bearing

material. The low toughness of magnesium has limited the use of these materials in engineering structures which makes it an ideal candidate for the matrix material in the self-healing alloy composite. The results of the design of a high performance composite will be presented elsewhere.

#### ACKNOWLEDGEMENTS

The authors would like to thank the following institutions for their financial support: Honeywell, National Aeronautics and Space Administration, and the National Academies. In addition, the authors are grateful to Professor Cate Brinson for her insight and the use of her laboratory facilities.

#### REFERENCE

1. Dry, C., *Matrix Cracking Repair and Filling Using Active and Passive Modes for Smart Timed Release of Chemicals from Fibers into Cement Matrices*. Smart Materials & Structures, 1994. **3**: p. 118-123.
2. Li, V.C., Y.M. Lim, and Y.W. Chan, *Feasibility study of a passive smart self-healing cementitious composite*. Composites Part B-Engineering, 1998. **29**(6): p. 819-827.
3. White, S.R., et al., *Autonomic healing of polymer composites*. Nature, 2001. **409**(6822): p. 794-797.
4. Files, B. and G. Olson. *Terminator 3: Biomimetic Self-Healing Alloy Composite*. in *SMST-97: Proceedings of the Second International Conference on Shape Memory and Superelastic Technologies*. 1997. Pacific Grove, California: The International Organization on Shape Memory and Superelastic Technologies (SMST).
5. Bruck, H.A., J.J. Evans, and M.L. Peterson, *The Role of Mechanics in Biological and Biologically Inspired Materials*. Experimental Mechanics, 2002. **42**(4): p. 361-371.
6. Zhou, B.L., *Bio-Inspired Study of Structural Materials*. Materials Science and Engineering C, 2000. **11**: p. 13-18.
7. Sarikaya, M. and I.A. Aksay, *Biomimetics : design and processing of materials*. AIP series in polymers and complex materials. 1995, Woodbury, N.Y.: AIP Press. xi, 285 , [4] of plates.
8. Feng, Q.L., et al., *Crystal Orientation, Toughening Mechanisms and a Mimic of Nacre*. Materials Science and Engineering C, 2000. **11**: p. 19-25.
9. Olson, G.B. and H. Hartman, *Martensite and Life - Displacive Transformations as Biological Processes*. Journal De Physique, 1982. **43**(NC-4): p. 855-865.
10. Olson, G.B., *Computational design of hierarchically structured materials*. Science, 1997. **277**(5330): p. 1237-1242.
11. Burton, D.S., X. Gao, and L.C. Brinson, *Finite element simulation of a self-healing shape memory alloy composite*. Mechanics of Materials, 2006. **38**(5-6): p. 525-537.
12. Brinson, L.C., *One-Dimensional Constitutive Behavior of Shape Memory Alloys: Thermomechanical Derivation with Non-Constant Material Functions and Redefined Martensite Internal Variable*. Journal of Intelligent Material Systems and Structures, 1993. **4**: p. 229-242.
13. Perkins, J., *Ti-Ni and Ti-Ni-X Shape Memory Alloys*. Metals Forum, 1981. **4**(3): p. 153-163.
14. Perkins, J., *Shape Memory Behavior and Thermoelastic Martensitic Transformations*. Materials Science and Engineering, 1981. **51**: p. 181-192.
15. Madangopal, K., G.R. Krishnan, and S. Banerjee, *Reversion Stresses in Ni-Ti Shape Memory Alloys*. Scripta Metallurgica, 1988. **22**(10): p. 1593-1598.

List of Figures

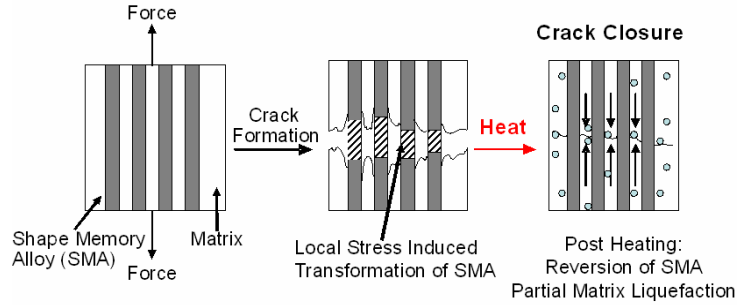


Figure 1. Schematic overview of the self-healing process

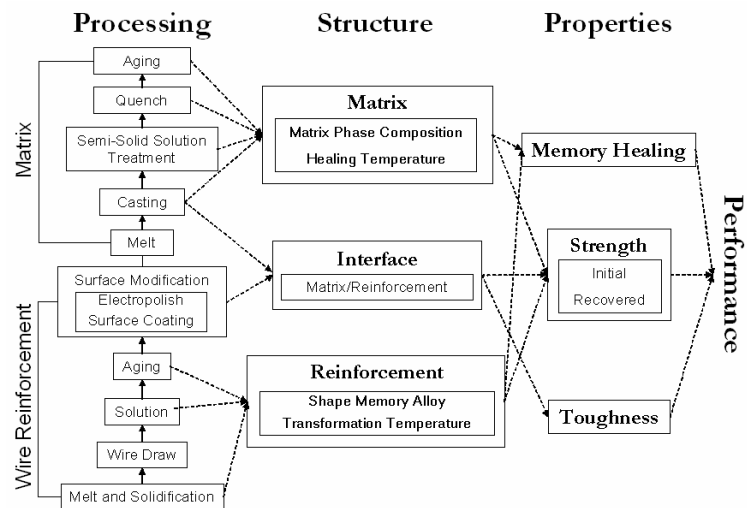


Figure 2. Self-healing alloy composite systems design chart.

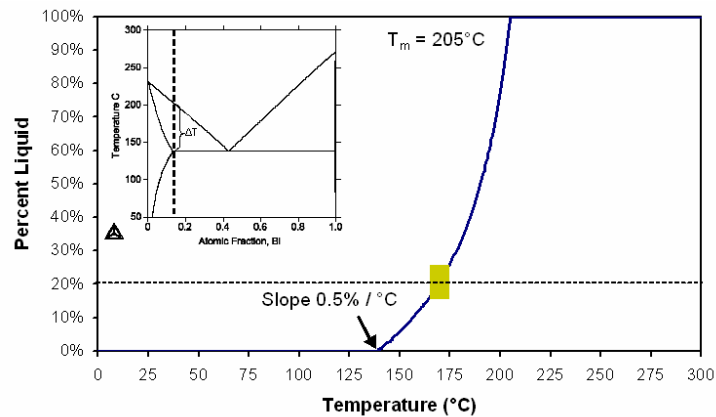


Figure 3. Phase diagram of the Sn-Bi alloy system indicating the composition used for the matrix and the fraction of liquid versus temperature curve displaying gradual melting behavior at healing temperature of 169°C.

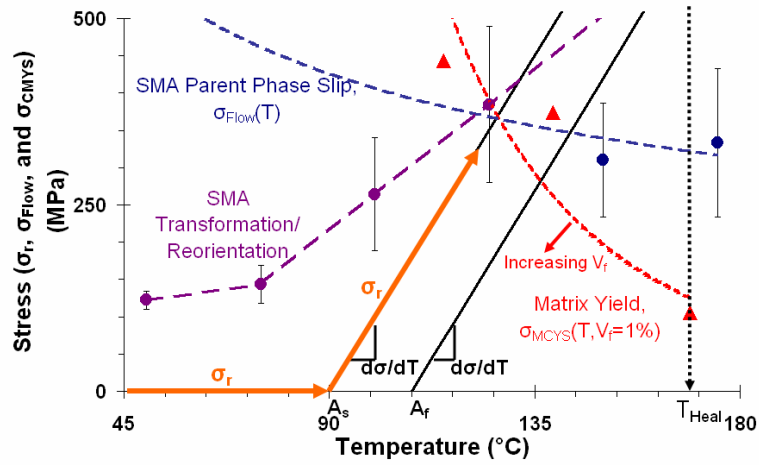


Figure 4. Stress versus temperature plot illustrating the evolution of reversion stress in the SMA wire as a function of temperature.

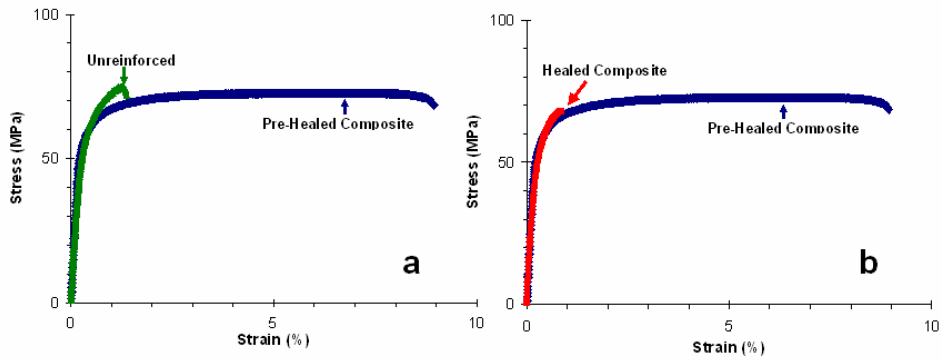


Figure 5. a) Comparison of stress-strain curves of the unreinforced matrix alloy and SMA reinforced composite ( $V_f=1\%$ ). b) Comparison of typical stress-strain curves of an pre-healed ( $V_f=1\%$ ) and healed composite ( $V_f=1\%$ ).

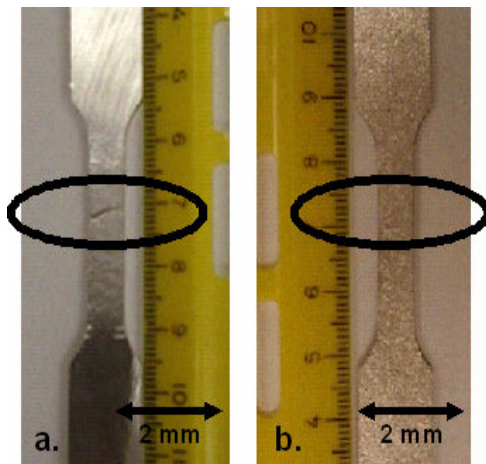


Figure 6. a) Demonstration of a pre-healed composite with a through matrix crack. b) Demonstration of a healed composite.